

	001
	002
	003
	004
	005
DRONE2REPORT: fast drone image processing for	006
precision agriculture	007
	008
	009
	010
Nelson Nazzicari <sup>1*</sup> , Giulia Moscatelli <sup>2</sup> , Agostino Fricano <sup>3</sup> ,	011
Elisabetta Frascaroli <sup>4</sup> , Roshan Paudel <sup>4</sup> , Eder Groli <sup>5</sup> ,	012
Paolo De Franceschi <sup>5</sup> , Giorgia Carletti <sup>3</sup> , Filippo Biscarini <sup>2</sup>	013
	014
<sup>1</sup> Research Centre for Animal Production and Aquaculture, Council for	015
Agricultural Research and Analysis of Agricultural Economics, Viale	016
Piacenza, 29, Lodi, 26900, Italy.	017
<sup>2</sup> Institute of Biology and Biotechnology in Agriculture (IBBA), National	018
Research Council (CNR), Via A. Corti, 12, Milan, 20133, Italy.	019
<sup>3</sup> Research Centre for Genomics and Bioinformatics, Council for	020
Agricultural Research and Analysis of Agricultural Economics, Via San	021
Protaso 69, Fiorenzuola d'Arda, 29017, Italy.	022
<sup>4</sup> Department of Agricultural and Food Sciences, University of Bologna,	023
Via G. Fanin, 44, Bologna, 40127, Italy.	024
<sup>5</sup> Research & Development, SIS - Società Italiana Sementi, Via	025
Mirandola, 5, San Lazzaro di Savena (BO), 40068, Italy.	026
	027
	028
	029
	030
*Corresponding author(s). E-mail(s): <a href="mailto:nelson.nazzicari@crea.gov.it">nelson.nazzicari@crea.gov.it</a> ;	031
Contributing authors: <a href="mailto:giulia.moscatelli@ibba.cnr.it">giulia.moscatelli@ibba.cnr.it</a> ;	032
<a href="mailto:agostino.fricano@crea.gov.it">agostino.fricano@crea.gov.it</a> ; <a href="mailto:elisabetta.frascaroli@unibo.it">elisabetta.frascaroli@unibo.it</a> ;	033
<a href="mailto:roshan.paudel@unibo.it">roshan.paudel@unibo.it</a> ; <a href="mailto:e.groli@sisonweb.com">e.groli@sisonweb.com</a> ;	034
<a href="mailto:p.defranceschi@sisonweb.com">p.defranceschi@sisonweb.com</a> ; <a href="mailto:giorgia.carletti@crea.gov.it">giorgia.carletti@crea.gov.it</a> ;	035
<a href="mailto:filippo.biscarini@cnr.it">filippo.biscarini@cnr.it</a> ;	036
	037
	038
<b>Abstract</b>	039
<b>Background</b> Unmanned aerial vehicles (UAVs) have become indispensable	040
tools in precision agriculture and plant phenotyping, enabling rapid, non-	041
destructive assessment of crop traits across space and time. Equipped with RGB,	042
multispectral, thermal, and other sensors, UAVs provide detailed information on	043
canopy structure, physiology, and stress responses that can guide management	044
	045
	046

047 decisions and accelerate breeding programs. Despite these advances, the down-  
048 stream processing of UAV imagery remains technically demanding. Converting  
049 orthophotos into standardized, biologically meaningful data often requires a com-  
050 bination of photogrammetry, geospatial analysis, and custom scripting, which can  
051 limit reproducibility and accessibility across research groups.

052 **Results** We present DRONE2REPORT, an open-source python-based software  
053 that processes orthophotos from UAV flights to generate vegetation indices, sum-  
054 mary statistics, and visual reports, supporting both research and applied breeding  
055 contexts. Alongside the basic structure and functioning of DRONE2REPORT, we  
056 present also four case studies that illustrate practical applications common in  
057 UAV/drone-phenotyping of plants: i) thresholding to remove background noise  
058 and highlight regions of interest; ii) monitoring plant phenotypes over time; iii)  
059 extracting information on plant height to detect events like lodging; iv) integrat-  
060 ing multiple sensors (cameras) to construct and optimise new synthetic indices.  
061 These examples demonstrate the tool's ability to automate analysis, integrate het-  
062 erogeneous data, and support reproducible computation of agronomically relevant  
063 traits.

064 **Conclusions** DRONE2REPORT streamlines UAV image processing for precision  
065 agriculture by linking orthophoto data to standardized, plot-level outputs. Its  
066 modular, configuration-driven design allows transparent workflows, easy cus-  
067 tomization, and integration of multiple sensors within a unified analytical frame-  
068 work. By facilitating reproducible, multi-modal image analysis, drone2report  
069 lowers technical barriers to UAV-based phenotyping and opens the way to robust,  
070 data-driven crop monitoring and breeding applications.

071 **Keywords:** drone phenotyping, image processing, software package, precision  
072 agriculture, UAV, vegetation index, NDVI

## 073 074 075 **Introduction**

076 Advances in precision agriculture and plant phenotyping increasingly rely on high-  
077 throughput, non-destructive methods for measuring crop performance under field  
078 conditions. Remote sensing platforms have become central to this effort, providing  
079 quantitative information on canopy structure, physiology, and stress responses. Among  
080 them, unmanned aerial vehicles (UAVs, or drones) are especially attractive due to their  
081 flexibility, affordability, and ability to generate repeated observations at plot or field  
082 scale. UAV-mounted sensors—ranging from RGB cameras to multispectral, thermal,  
083 and LIDAR (Laser Imaging, Detection, And Ranging) units—enable detailed mea-  
084 surement of vegetation indices, canopy temperature, and topography that can inform  
085 breeding programs and management decisions [1].

086 Although the potential of UAV imagery for plant science is well recognized, the  
087 software ecosystem supporting its analysis remains fragmented. Many researchers  
088 rely on commercial photogrammetry suites for orthomosaic production, followed by  
089 manual processing in GIS software or custom scripts for index calculation and region-  
090 of-interest (ROI) extraction. This workflow can be labor-intensive, error-prone, and  
091

difficult to reproduce across experiments or research groups. Existing open-source solutions are usually not designed for agriculture applications (e.g. [2]), have sometimes very specific targets (e.g. seeds [3], berries [4]), focus on single data types (e.g. RGB or multispectral), provide limited support for multi-modal datasets, or lack transparent configuration and automation mechanisms. As UAV datasets grow in size and complexity, there is a growing need for tools that combine reproducibility, flexibility, and ease of use, while remaining accessible to plant researchers without advanced programming expertise. DRONE2REPORT was developed to address this gap. It is designed specifically for agriculture (*e.g.* a field with multiple plots each accommodating one genotype) and implements a configuration-driven pipeline that streamlines the transformation of UAV imagery into standardized outputs—such as vegetation indices, ROI-based statistics, and summary reports—across multiple sensor types. By emphasizing reproducibility, modularity, and compatibility with common research workflows, DRONE2REPORT aims to lower the barrier to adoption of UAV-based phenotyping and facilitate robust comparisons across experiments, genotypes, and environments. The software is released under open-source license and readily available at <https://github.com/ne1s0n/drone2report>. In this paper, we present the technical details of this new tool, followed by four case-studies describing examples of its application, a comparison with other available software packages, and a discussion of the merits, limitations and future expansions of DRONE2REPORT.

## Methods

### Data workflow

The general workflow of DRONE2REPORT is reported in Figure 1. The first step is data acquisition, with the drone(s) flying over the field of interest and collecting a series of overlapping images, which are then collated together into what is called an orthophoto (or orthomosaic, or orthorectified image). This computational step produces a georeferenced composite image and corrects for several technical issues such as perspective distortion, map projection, and lens aberrations. The generation of orthophotos is now considered a well-established process, thanks to the availability of mature open-source tools such as OpenDroneMap [5], MicMac [6], and QGIS [2]. Together with the orthorectified image (typically in the .tif format), a digital elevation model (DEM) file is also produced, which describes the three-dimensional structure of the field.

In a typical agricultural application, several flights are performed over the same field during a growing season. In fact, the flights may start on the empty field just after sowing, so that the first orthophoto and DEM file represent the baseline for all successive flights. On this empty field, a "shape file" is traced, containing the shapes and placements of all regions of interest (ROIs). Typically, each plot becomes a ROI, with the edge case of the entire field comprised of a single ROI. Defining ROIs is essential, because the area scanned by the drone is always larger than the actual target field surface and typically covers borders, utility roads and other external elements.

Orthophotos are typically multichannel images, with common cases being three channels (visible RGB spectrum), while multispectral images may include additional

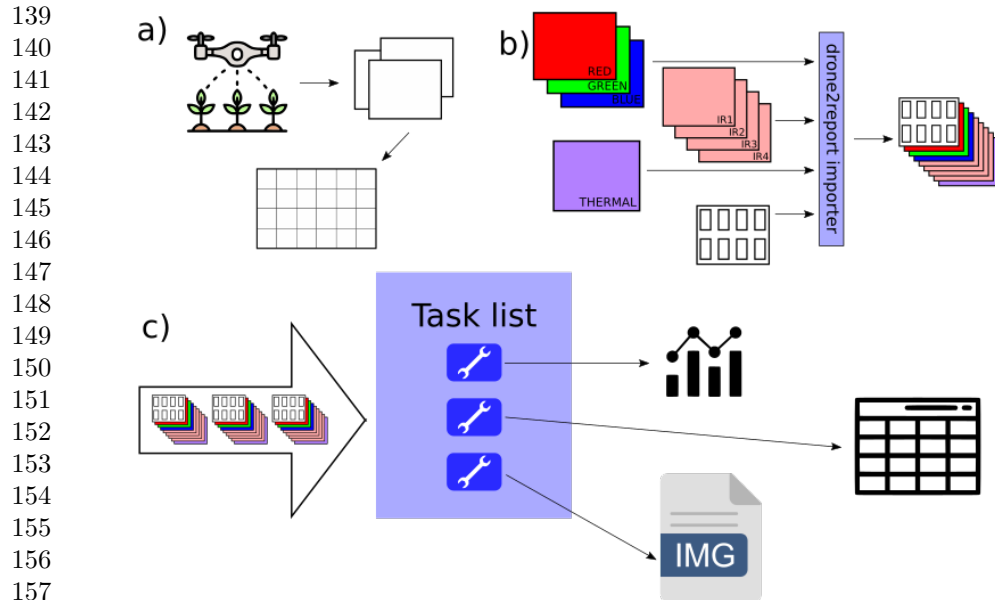


**Fig. 1** General application workflow. Panel a: drones capture raw, partial images of the field (depending on the mounted sensors). All images from a single flight are collated in a unique orthophoto. Panel b: orthophotos coming from one or more sensors, together with a shape file that specifies the ROIs, enter DRONE2REPORT and are converted to an internal *dataset* object. Panel c: all datasets are inputed, in turn, to all queued tasks, each task producing its specific output (e.g. tables, other images etc.)

bands, such as near-infrared (NIR). Thermal data is encoded as a single channel and possibly rendered as grayscale images, with each pixel corresponding to a single temperature read. Even elevation models (DEM files) can at this stage be considered as a valid data input: a single channel image where each pixel corresponds to a measured height.

DRONE2REPORT can receive as input one or more orthophotos. If more than one image is provided, they will be internally stacked into a new multichannel image called *dataset*. For example, providing an RGB image plus a thermal image will create a four-channels RGBT *dataset*. Differences in image sizes and resolutions are solved via interpolation and taking into account possible differences in georeferencing data. This results in the creation of a single tensor-like data structure with a single shape (width and length) and as many channels as the sum of all input images channels. This unified representation enables to perform algebraic operations on all combined channels simultaneously, and even combine data coming from different flights and sensors. Even when multiple orthophotos are combined into a *dataset* the ROIs are specified only once.

One *dataset* can thus be composed of several orthophotos, and several *datasets* can be loaded. DRONE2REPORT then proceeds to feed all the data to a queue of tasks. As of the current implementation, a number of tasks is implemented for computing

various vegetation indices, rescaling and extracting subimages, and preparing data for successive elaboration (*e. g.* training neural networks). 185  
186

## Software implementation 187

DRONE2REPORT is a Python-based, open source, free software. It is written to be integrated in standard elaboration pipelines aimed to agricultural drone images, both for research and industrial applications. As such, it has no GUI and runs, ideally server-side, on data files and configuration (.ini) files. It has an extensive logging functionality and can be used out of the box without any python coding. However, it is designed with modularity in mind, allowing for straightforward extension through the addition of new tasks. 188

An example configuration (.ini) file is provided in Box 2, demonstrating how to compute two vegetation indices from a single RGB image. The basic structure of the configuration file includes three main sections: i) DEFAULT specifies base parameters like the input and output folders, the number of cores (processing units) to be used, and whether a verbose output log is desired; ii) DATA specifies the image file name (with some metadata, *i.e.* date, description etc.), its type (only tif\_multichannel is currently supported), the value that indicates missing pixel data (*e.g.* -1), the channels (total and visible), the maximum pixel intensity value, the path to the shape file; iii) TASK specifies which vegetation indices will be computed. More details on how to use DRONE2REPORT can be found in the on-line documentation (<https://drone2report.readthedocs.io/en/latest/>). Once the configuration file is ready, DRONE2REPORT will be run from the shell command line. 189

The modularity of DRONE2REPORT can be leveraged at several levels. The easiest customization would be to add new specialized vegetation indices to the proper python file (*e.g.* `matrix_returning_indices.py` file in the folder `/drone2report/d2r/tasks/` from the github repository). Listing 1 reports an example of such a function. 190

A more powerful intervention consists of designing a new TASK, which will then require its own section in the .ini file. For that purpose, a TASK template is provided. Finally, new types of DATA could be supported, which would require some care to curate the exposed functionalities. 191

192  
193  
194  
195  
196  
197  
198  
199  
200  
201  
202  
203  
204  
205  
206  
207  
208  
209  
210  
211  
212  
213  
214  
215  
216  
217  
218  
219  
220  
221  
222  
223  
224  
225  
226  
227  
228  
229  
230

231     **Listing 1** Example of function computing the GLI vegetation index on a passed image  
232

```
233     def GLI(img, channels):
234         """Green leaf index, uses red, green, blue channels"""
235         try:
236             red    = img[:, :, channels.index('red')]
237             green = img[:, :, channels.index('green')]
238             blue   = img[:, :, channels.index('blue')]
239
240         except ValueError:
241             return np.nan
242
243         return(
244             (2.0*green - red - blue) /
245             (2.0*green + red + blue)
246         )
```

247  
248     New indices and functionality can be proposed and eventually integrated in the  
249 main software codebase via Github pull requests.

250     Note that DRONE2REPORT anticipates the most common needs of agricultural  
251 experiments. For example, when a vegetation index is computed, the software already  
252 summarizes it through a series of descriptive statistics, which are collated and saved  
253 in tabular format.

254     Internally, DRONE2REPORT uses the GDAL [7] and geopandas [8] libraries for  
255 manipulation of georeferenced images. DRONE2REPORT is released with a custom  
256 Conda environment for multi-platform installation.

257     The DRONE2REPORT open-source code is available on-line in the following Github  
258 repository: <https://github.com/ne1s0n/drone2report>.

259  
260  
261  
262  
263  
264  
265  
266  
267  
268  
269  
270  
271  
272  
273  
274  
275  
276

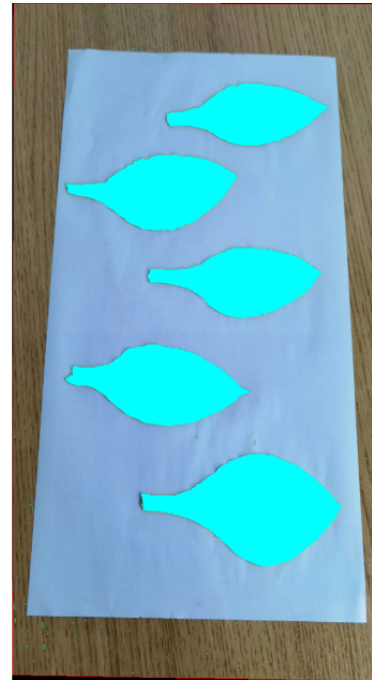
<b>Listing 2</b> Example of configuration .ini file to run drone2report	277 278 279 280 281 282 283 284 285 286 287 288 289 290 291 292 293 294 295 296 297 298 299 300 301 302 303 304 305 306 307 308 309 310 311 312 313 314 315 316 317 318 319 320 321 322
<pre>[DEFAULT] infolder=&lt;/base/folder&gt; outfolder=&lt;/output/folder&gt; cores=4 skip_if_already_done=False verbose=True  [DATA image] active=True meta_date=2024/03/25 meta_time=1.45 pm meta_desc=Barley field barley , March 2024, RGB flight type=tif_multichannel orthomosaic=\${DEFAULT:infolder}/&lt;img-name.ext&gt; channels=red , green , blue visible_channels=red , green , blue max_value=255 nodata=-1 shapes_file=\${DEFAULT:infolder}/&lt;img.shp&gt; shapes_index=id  [TASK indices] active=True outfolder=\${DEFAULT:outfolder}/&lt;results&gt; indices=GLI,HUE</pre>	

## Results

To illustrate how to use DRONE2REPORT for image processing from drone phenotyping, and to show some potential and useful applications of vegetation indices, we present four case studies: i) thresholding; ii) evolution of vegetation indices over time; iii) detection of lodging; iv) combining multiple sensors and index optimization.

### Case study n. 1: thresholding

In the first case study we use DRONE2REPORT to calculate a vegetation index after applying different value thresholds to highlight the regions of interest. Thresholding can be useful to remove alien elements from the computation. In a typical case, it is desirable to compute a vegetation index only on the areas actually covered by plants, excluding the soil. In this example we compute the Green Leaf Index (GLI), whose positive values tend to identify green vegetation (e.g. leaves and stems), while negative values tend to reflect soil/non-vegetation [9]. Our objective might be to calculate the

323   **A**324   **B**

344   **Fig. 2** Example RGB image of tobacco leaves (*Nicotiana tabacum*). A) The original image of the  
 345   tobacco leaves as downloaded from <https://www.dropbox.com/s/is4jrmlmmcfpdः?dl=1>; B) The same image with threshold 0.1: the pixels highlighted in turquoise are those that will  
 346   be used for the calculations of the vegetation indices.  
 347

348   proportion of vegetation to soil, or to compare the green intensity of different fields or  
 349   over time. In both cases, we may want to remove the image background (i.e. “noise”,  
 350   like a road, a pond or just bare soil) which can be achieved via thresholding [10].

352   To illustrate the removal of background noise, we use one RGB image of  
 353   tobacco leaves from the Github repository (<https://github.com/tanghaibao/jcvi/wiki/GRABSEEDS>) of the GRABSEED software [3] (see Figure 2)

355   In this example, our objective is to calculate the GLI vegetation index for the  
 356   tobacco leaves. GLI is computed per-pixel using the following formula:

$$357 \quad 358 \quad \text{GLI}(\mathbf{p}) = \frac{(2 \cdot p_{green} - p_{red} - p_{blue})}{(2 \cdot p_{green} + p_{red} + p_{blue})} \quad (1)$$

359

360   where  $\mathbf{p} := [p_{red}, p_{green}, p_{blue}]$  is a single pixel of an RGB image and contains the  
 361   normalized intensities of the three channels.

362   With reference to Figure 2, the aim is to remove the background table (brownish)  
 363   and the light-blue paper-cloth from the calculation. As a first step, we computed  
 364   GLI on the image and obtained the distribution reported in Figure 3. The image  
 365   highlights two clear clusters, one around zero, the other larger than 0.2. These two  
 366   groups correspond to the non-leaf background and to the tobacco leaves, with different  
 367   intensities of green. Thus, a threshold of 0.1 would separate the two clusters. This value  
 368   is incorporated when invoking DRONE2REPORT [TASK index]. We obtain a resulting

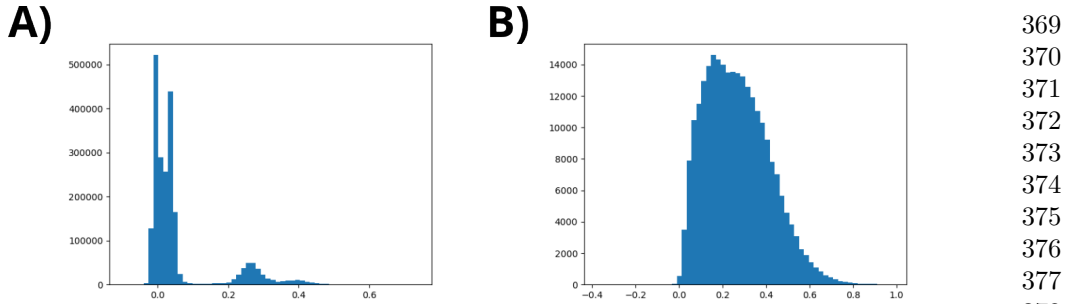


**Fig. 3** Distribution of values for the vegetation index GLI (Green Leaf Index) for: A) the tobacco leaves image; and B) for the barley field plot image

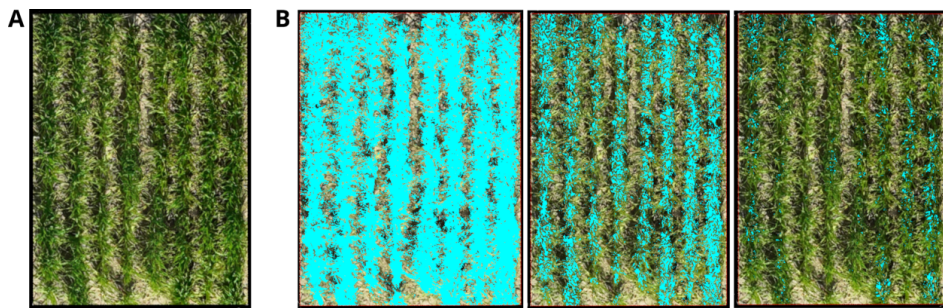


**Fig. 4** Example RGB image of one single barley field plot. A) The original image of the barley field: all pixels would be used for index calculations; B) The same plot with increasing thresholds for the index values: 0.2, 0.4, 0.6 (rescaled in [0, 1]). As the threshold is increased, fewer and fewer pixels are used for the calculations of the index (indicated in turquoise).

GLI average value of  $0.289 \pm 0.07$ , calculated only from the leaves. If we apply the same procedure to other images of tobacco leaves, we can then compare the corresponding GLI values.

In a more realistic case the GLI values clusters from different segments of the image may not be as clear as in the tobacco-leaves example. An example is reported in Figure 4, panel A: a drone-captured RGB image of a single plot from a barley field in Fiorenzuola d'Arda (PC), Italy,  $44^{\circ}55'27''N, 9^{\circ}54'47''E$ , taken on March 25th 2024 (“Polyplloidbreeding” research project: <https://polyplloidbreeding.ibba.cnr.it/>). For this image, the distribution of GLI index values is unimodal (no clusters: Figure 3, panel B).

In such a case, no clear-cut threshold could possibly separate all background pixels. We used DRONE2REPORT [TASK thumbnail] to generate copies of the original image with increasing GLI thresholds: from 0.1 to 1 (Figure 4, panel B, shows the image with thresholds 0.2, 0.4 and 0.6). We then calculated the GLI index using only the pixels above the threshold, from the original image (no threshold, all pixels used), to the maximum 0.9 threshold. The DRONE2REPORT [TASK index] was used for index

369  
370  
371  
372  
373  
374  
375  
376  
377  
378  
379  
380  
381  
382  
383  
384  
385  
386  
387  
388  
389  
390  
391  
392  
393  
394  
395  
396  
397  
398  
399  
400  
401  
402  
403  
404  
405  
406  
407  
408  
409  
410  
411  
412  
413  
414

415	<b>threshold</b>	<b>pixels</b>	<b>after_th</b>	<b>GLI_mean</b>	<b>GLI_med</b>	<b>GLI_std</b>	<b>GLI_max</b>	<b>GLI_min</b>
416	none	254493	254493	0.26837	0.25397	0.14712	0.97753	-0.36842
417	(GLI >0.0)	254493	254251	0.26866	0.25424	0.14690	0.97753	0.00000
418	(GLI >0.1)	254493	222159	0.29813	0.28090	0.13327	0.97753	0.10000
419	(GLI >0.2)	254493	160082	0.35525	0.33333	0.11271	0.97753	0.20000
420	(GLI >0.3)	254493	99914	0.41901	0.39706	0.09542	0.97753	0.30000
421	(GLI >0.4)	254493	48731	0.49456	0.47200	0.08247	0.97753	0.40000
422	(GLI >0.5)	254493	18278	0.58052	0.55932	0.07340	0.97753	0.50000
423	(GLI >0.6)	254493	5799	0.67194	0.65289	0.06573	0.97753	0.60000
424	(GLI >0.7)	254493	1860	0.76379	0.74713	0.05775	0.97753	0.70000
425	(GLI >0.8)	254493	798	0.85531	0.84240	0.04428	0.97753	0.80000
426	(GLI >0.9)	254493	558	0.93064	0.92203	0.02319	0.97753	0.90164

**Table 1** Green leaf index (GLI) values with different thresholding, as computed by [TASK index]. For each Region Of Interest (as defined in the shapefile) a set of summary statistics is computed for each index (mean, standard deviation, min and max). after\_th: n. of pixels left for the calculation after thresholding

427 .

428 .

429 calculations, each time specifying the corresponding threshold (if any). Results are  
430 shown in Table 1.

431 We see that the number of pixels used decreases with the threshold used. Not  
432 surprisingly, given that GLI measures the green intensity of pixels in the image, GLI  
433 values increase with the threshold, from 0.26 to 0.93: essentially, since Figure 4 (A) is  
434 a barley field, we are progressively getting rid of the soil and of the less green parts  
435 of the plants. Depending on the application, it may be desirable to focus only on  
436 vegetation, or even on the plants' greenest parts. In contrast, it may be acceptable  
437 to remove only pixels with negative GLI values (GLI > 0.0), which are definitely not  
438 green. This is reported in Table 1, second row.

439 Note that in these examples, for simplicity, we applied thresholding on the same  
440 index that was computed. However, it is possible to threshold the image based on one  
441 index and then compute one (or more) other indices on the retained pixels in a single  
442 pass. Moreover, it is also possible to specify more complex thresholding, e.g. banding,  
443 such as (GLI > 0)  $\wedge$  (GLI < 0.8).

#### 445 Case study n. 2: monitoring vegetation indices over time

446 In this case study, we use DRONE2REPORT to monitor the evolution of vegetation  
447 indices over time. This is the case when several images of the same field/area are col-  
448 lected at successive time intervals, *e.g.* for a phenotyping experiment in plant breeding.  
449 Vegetation indices over time may be useful to monitor plant growth, soil coverage,  
450 maturation etc. over a period of time of interest, like a growing season.

451 In this illustration, drone-captured barley-field images from the same experiment as  
452 in case study n. 1 were used. However, instead of using one single plot (one single barley  
453 variety), the images cover 20 plots (20 barley varieties) for 10 flights. For vegetation  
454 indices, we use GLI (described before, see Formula 1) and HUE [11] defined as:

455

$$456 \quad 457 \quad \text{HUE}(\mathbf{p}) = \arctan \left( \frac{2 \cdot p_{red} - p_{green} - p_{blue}}{30.5} \cdot (p_{green} - p_{blue}) \right) \quad (2)$$

458

459

460

where  $\mathbf{p} := [p_{red}, p_{green}, p_{blue}]$  is a single pixel of an RGB image and contains the normalized intensities of the three channels. HUE too can be used to discriminate between vegetation and non-vegetation, e.g. soil vs plant, although it is more dependent on lighting, camera and background [12].

To calculate vegetation indices over multiple images (i.e. successive flights) for field/area using DRONE2REPORT we can follow two approaches: i) we can add several data sections in the configuration (.ini) file, one for each image, then run drone2report just once; or ii) iterate over the number of images, automatically generating each .ini file, thus running DRONE2REPORT as many times as there are images.

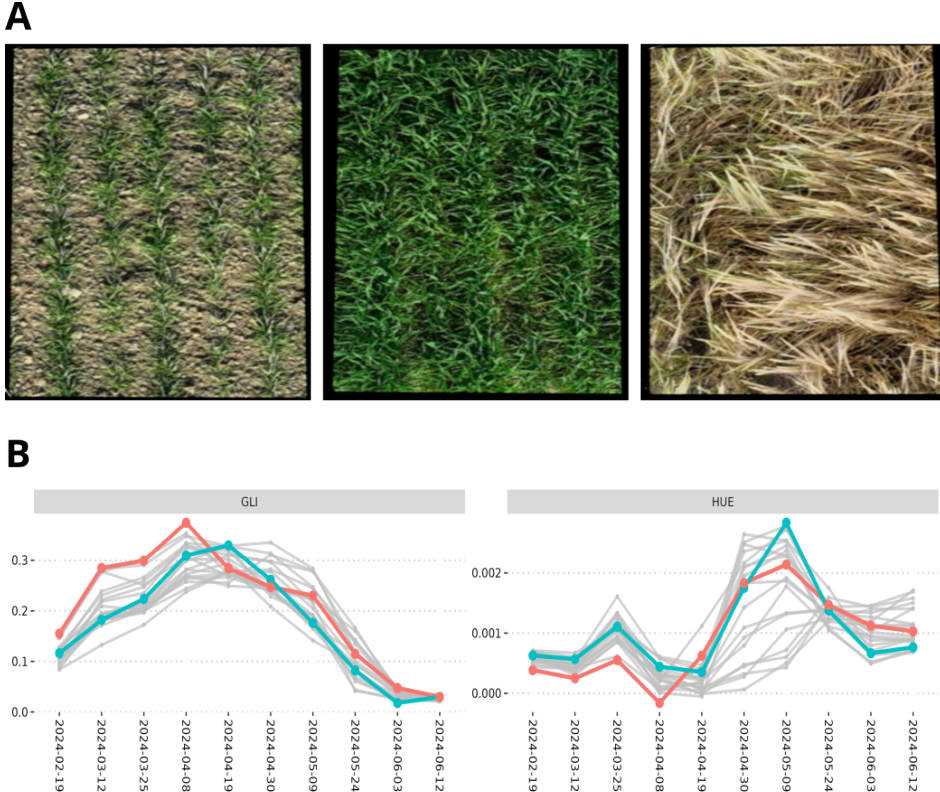


**Fig. 5** Vegetation indices over time. A) The same barley plot drone-photographed in February, April, and June. B) Evolution of GLI index (left) and HUE index (right) values for twenty barley varieties over the entire growing season (10 flights in February-June 2024). Two arbitrary selected varieties are highlighted (red and blue).

Once the chosen vegetation indices are computed for all multiple images, it is possible to plot the trends over time to monitor the evolution of the field. In the barley field example each plot represents a different variety. It is thus possible to also implement inter-varietal comparisons. This is shown in Figure 5 (B), where we highlighted two arbitrary varieties (in red and blue). The barley plots are shown to

507 start with moderate green intensity (sparse vegetation), reach a maximum around  
508 April to early May (thick vegetation), then decrease toward the end of the growing  
509 season (matured yellowish barley in June). This trend matches what we observed in  
510 the RGB images (Figure 5, A). The two indexes follow a similar trend, with a peak  
511 and a decrease. Interestingly, GLI peaks earlier than HUE, which in turn shows a  
512 sharper peak around May. The indexes also show variability between the different  
513 barley varieties, linked to their different genetic background.

514

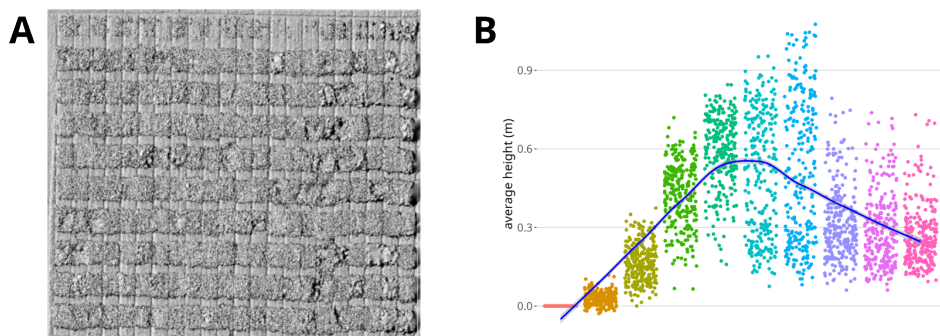
### 515 Case study n. 3: detecting lodging from DEM files

516

517 As mentioned before, drone phenotyping produces also a DEM file alongside the ortho-  
518 mosaic image. DEM files report the height of each pixel in the orthomosaic image: this  
519 height is usually reported in meters, and is measured from a reference ellipsoid. Given  
520 that the first flight it is usually done on an empty field, it can be used as reference.  
521 By subtracting the heights from the first flight from all successive flights it is possible  
522 to estimate the growth heights.

523 In Figure 6, A, it is reported a hill-shade rendering of a DEM file for the example  
524 barley field (part of it) to visualize the 3D structure of the field image. Pixel heights  
525 will differ depending on the content, being soil, an erect plant, or a lodged one. The  
526 evolution of per-plot average heights is reported in Figure 6 (B) for the successive  
527 flights. Note that the very first flight is used as reference and thus all pixels are zero  
528 by definition.

529



541 **Fig. 6** Example .dem file of a barley field (left: flight on 19/04/2024); plant height (metres) calculated  
542 from the .dem file by drone2report, over 10 flights covering the growing season (right).

543

544 After the first flight the heights quickly increase up to the 5th-6th flight (mid-April:  
545 the plants were growing). In our barley field trials, DRONE2REPORT shows a decrease  
546 of height after the 7th flight due to lodging, consistently with the genetic material  
547 examined (old cultivars and landraces) and the adverse weather conditions. This can  
548 also be visually confirmed examining the right-most part of Figure 5 (A), where a  
549 large portion of barley plants appears to have been flattened. Therefore, we can see  
550 that the analysis of DEM files allowed us to detect if and when lodging occurred in  
551 our field of interest.

552

It is also possible to estimate the per-plot volumes using DRONE2REPORT. Consider  
 that the integral of an area is proportional to the sum of the heights of each pixel.  
 When computing indexes like GLI or HUE the actual result of the computation is  
 a matrix with exactly the same dimension as the ROI (i.e. the plot). It is however  
 possible to select "indexes" that return a single scalar number, e.g. the summation of  
 all values of the DEM file for a plot. This serves as a numeric approximation of the  
 volume, which in turn could be used to estimate crop yield or biomass.

## Case study n. 4: merging images from multiple sensors and index optimization

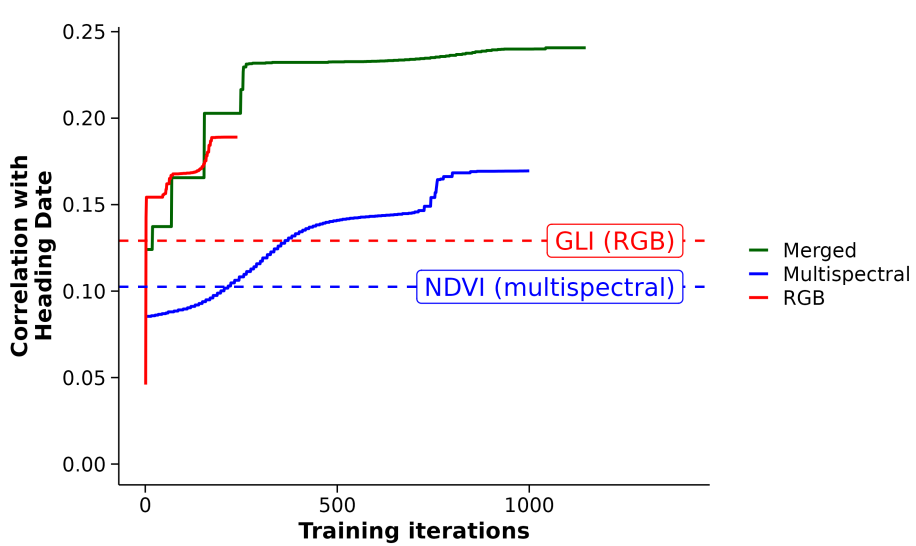
DRONE2REPORT can transparently import images from different sensors and merge  
 them into a single data structure where all channels of the original images are stacked.  
 For example, it is possible to merge images coming from visible wavelength (e.g. RGB  
 images), from multispectral sensors (e.g. infra-red and near-infra-red images) and from  
 a thermal camera. Differences in image resolutions are managed automatically via  
 interpolation, and differences in spatial reference system (SRS) are handled via repro-  
 jection. The resulting data structure exposes, for each pixel, a number of channels  
 equal to the sum of all channels of the original images. Thus, it is possible to leverage  
 different data sources together and transparently.

In this case study three images are merged: one RGB (three bands), one multi-  
 spectral (ten bands) and one thermal (one band). All images are of a barley field close  
 to harvesting time. The field is structured in 264 plots, each phenotyped for heading  
 date, i.e. the number of days from sowing when the spike (head) has emerged from  
 the flag leaf sheath in 50% of the plants in a plot. The aim of of this case study is to  
 optimize a new vegetation index of the form:

$$I(\mathbf{p}) = \frac{n_0 + \sum_{i=1}^{14} n_i p_i}{d_0 + \sum_{i=1}^{14} d_i p_i} \quad (3)$$

where  $\mathbf{p} \in \mathbb{R}^{14}$  is a pixel on the merged 14-bands image. The set of 30 coefficients  
 $[n_0, \dots, n_{14}, d_0, \dots, d_{14}]$  are to be chosen to maximize the Pearson's correlation between  
 the array of heading dates and the array of per-plot average index values. Formula 3  
 is designed as a generalization of the most commonly used indices such as NDVI, GLI,  
 VARI, etc.[13].

This thus becomes a 30-parameters optimization problem, which can be solved  
 via a new custom DRONE2REPORT task. Internally, the task uses Scipy's [14] *optimize.minimize()* function based on the *Nelder-Mead* numerical method [15]. The  
 results of the optimization process are reported in Figure 5, which shows the optimiza-  
 tion trajectory of the custom index in equation 3 through all training iterations.  
 The index was optimized on the merged 14-bands image and, for comparison, on  
 both the visible RGB image and the 10-bands multispectral image, separately.  
 Additionally, the plot also reports the Pearson's correlation with heading date for  
 the two best performing vegetation indices among the twenty one currently imple-  
 mented in DRONE2REPORT, namely NDVI (Normalized Difference Vegetation Index,  
 for multispectral images) and GLI (Green Leaf Index, for RGB images).



619 **Fig. 7** Optimization trajectories through training cycles. The custom index described in Formula 3  
 620 was optimized for maximal Pearson's correlation between the vector of its per-plot averages and the  
 621 phenotype *heading date*. Solid lines show three optimization trajectories on different input images,  
 622 namely RGB, 10-bands multispectral, and a 14-bands merged image containing RGB, multispectral  
 623 and temperature data. For reference, the two best performing indices (NDVI and GLI) are also  
 624 reported.

625 The results show that it is possible to optimize a custom vegetation index on a  
 626 specific drone dataset and beat the correlations of standard indices. The optimization  
 627 process is iterative and stochastic, so different images required different amounts of  
 628 iteration before converging. Optimizing on the RGB image required little more than  
 629 two hundred iterations, while on the 14-bands merged image it required 1148 iterations.  
 630 These numbers would change if the process were repeated and are influenced by  
 631 the initialization process, which assigns random values to the parameters. However, in  
 632 general a longer optimization process is expected the more parameters are to be tuned.

633 The indices obtained with this case study are likely overfitting, at least partially.  
 634 A focused, future study, could estimate the fraction of overfitting and apply  
 635 regularization techniques to ensure good generalization of the results.

## 636 Discussion

637 In this section, we first compare DRONE2REPORT to the state-of-the-art software tools  
 638 for drone-images processing in agriculture. Then we discuss the range of applications  
 639 of DRONE2REPORT, its strengths and limitations, and the future directions for further  
 640 developments.

<b>State of the art and positioning of drone2report</b>	645
UAV imagery has become central to high-throughput field phenotyping, with numerous reviews documenting rapid adoption across RGB, multispectral and thermal sensing for crop trait estimation and stress monitoring [16, 17]. These studies consistently highlight persistent bottlenecks not in image acquisition, but in the standardization and analysis of downstream workflows [18].	646
Several tools and software packages are available for processing and analysing UAV-acquired image data, including commercial products [19]. In this section, we briefly survey the most common open-source and/or freeware tools that are currently available for photogrammetric data processing, and describe where DRONE2REPORT stands in this landscape. The majority of open-source/freeware software packages for UAV-imagery processing is written in Python and based on libraries for image manipulation like <code>scikit-image</code> , <code>PIL/Pillow</code> , <code>GDAL</code> , <code>geopandas</code> .	647
<i>OpenDroneMap</i> (ODM/WebODM: <a href="https://github.com/OpenDroneMap/WebODM">https://github.com/OpenDroneMap/WebODM</a> , [20]) is a mature, subscription-based software stack that excels at turning raw images into geospatial products —orthomosaics, point clouds, 3D meshes and DEMs— and even provides “plant health” visualizations (e.g., NDVI/VARI) within the viewer. However, its focus is reconstruction; downstream plot-level analytics, multi-sensor alignment, and standardized per-ROI statistics/reporting fall largely outside its scope.	648
<i>Orfeo ToolBox</i> (OTB: <a href="https://gitlab.orfeo-toolbox.org/">https://gitlab.orfeo-toolbox.org/</a> , [21, 22]) is a general-purpose remote sensing library that offers state-of-the-art algorithms via command-line apps, Python bindings and QGIS integration, making it highly flexible for classification, segmentation and raster math. Yet OTB is intentionally low-level: users compose pipelines themselves and must implement domain-specific phenotyping logic (e.g., plot masks, trial layouts, multi-sensor co-registration, batch reporting).	649
<i>QGIS</i> ( <a href="https://qgis.org/">https://qgis.org/</a> , [2]) is a free and open-source desktop geographic information system (GIS) suite. It allows users to create, edit, visualize, analyze, and publish geospatial information. In particular, QGIS provides a Processing Modeler [23] for chaining algorithms and running them in batch, which can partially address reproducibility. In practice, model portability, parameter/version management, and experiment-level reporting remain challenging, especially across groups and compute environments.	650
<i>PlantCV</i> ( <a href="https://plantcv.org/">https://plantcv.org/</a> , [24]) is a widely used, open-source platform for modular image analysis in plant science, particularly effective for close-range/greenhouse imagery and single-image pipelines. It is commonly run using Jupyter notebooks. It is not primarily oriented to georeferenced orthomosaics, or plot-level analysis.	651
<i>GRABSEEDS</i> ( <a href="https://github.com/tanghaibao/jcvi/wiki/GRABSEEDS">https://github.com/tanghaibao/jcvi/wiki/GRABSEEDS</a> , [3]) is a command-line Python software tool specifically engineered for the identification and phenotyping of plant seeds, leaves and flowers. It performs edge detection, object (seed) identification, image cropping and text label recognition, across a wide range of grains and legumes. However, <i>GRABSEEDS</i> only accepts in input RGB image files, and is not designed to work with UAV-captured field image data.	652
	653
	654
	655
	656
	657
	658
	659
	660
	661
	662
	663
	664
	665
	666
	667
	668
	669
	670
	671
	672
	673
	674
	675
	676
	677
	678
	679
	680
	681
	682
	683
	684
	685
	686
	687
	688
	689
	690

691        *BerryPortraits* (<https://github.com/Breeding-Insight/BerryPortraits/>, [4]) is an  
692 open-source Python image-analysis software based on the YOLOv8 model for com-  
693 puter vision [25]. This is a command-line tool (no GUI), that detects and segments  
694 berries and extracts morphometric data on quality traits like berry color, size, shape,  
695 and uniformity. As other highly specialised tools, *Berryportraits* only works with RGB  
696 images and not with UAV aerial photogrammetry.

697        *FIELDImageR* (<https://github.com/OpenDroneMap/FIELDImageR>, [26]) is one of  
698 the very few software packages for UAV-imagery processing written in R. It targets  
699 orthomosaics from field trials and provides functions for plot extraction and vegetation  
700 indices, but is embedded in the R ecosystem and typically used through script-  
701 s/notebooks rather than a configuration-driven, sensor-agnostic CLI (command-line  
702 interface) designed for end-to-end, repeatable reports.

703        In contrast to the above solutions, DRONE2REPORT has been developed specifically  
704 to streamline the processing of UAV-captured images for the calculation of vegetation  
705 indices and the reporting of relevant summary statistics. It is designed to sit after the  
706 orthomosaic generation (e.g. from ODM/WebODM or commercial tools) and provides  
707 a configuration-driven, reproducible pipeline that takes in input and multiband image  
708 (being it RGB, multispectral, thermal images and DEM files). Its core functionalities  
709 include: i) identifying regions of interests (ROIs, based on the shape file); ii) calcu-  
710 lating vegetation indices; iii) thresholding; iv) summarising statistics; v) generating  
712 thumbnails. Moreover, the software is open source and freely (and easily) customizable.

713        The software is open-source, easily customizable, and designed for batch processing  
714 via a single configuration file (in .ini format). It runs entirely via the command line  
715 (no GUI dependency), ensuring platform independence and reproducibility across labs  
716 and servers. Dependencies are managed through a Conda environment, simplifying  
717 installation and portability.

718        A distinctive feature of DRONE2REPORT is its support for multi-sensor alignment  
719 and combined index generation, with built-in resampling and spatial reference sys-  
720 tem (SRS) management. This enables new analyses that leverage data from multiple  
721 sources—an emerging need in precision agriculture. Moreover, the tool emphasizes  
722 robust validation and reporting, with support for dry runs and standardized outputs  
723 per ROI, ready for integration into statistical workflows.

724        In short, while ODM/WebODM specializes in map making, OTB and QGIS  
725 provide low-level building blocks, GRABSEEDS and BerryPortraits occupy specific  
726 application niches, and PlantCV and FIELDImageR target image-centric or R-centric  
727 workflows, DRONE2REPORT contributes a domain-specific, geospatial, configuration-  
728 driven bridge from orthomosaics to plot-level, multi-sensor, repeatable reports tailored  
729 to field phenotyping.

730        **731 Applications, limitations and future developments**  
732        The main goal of DRONE2REPORT is to automate the calculation of vegetation indices  
733 from multi-channel UAV imagery—a key task in modern precision agriculture (e.g.  
734 [27–29]). We showed several case studies on how vegetation indices can be obtained and  
736

used for a range of applications including: removal of background noise via thresholding, comparison of different fields and/or plots; time-series analysis, lodging detection, development of novel indices through the optimization of multiple mixed channels for a target metric.	737
	738
	739
	740
The tool is easy to use from the command line by simply modifying the configuration file (several different templates are provided in the online documentation). It is also easily portable, on any OS or platforms where Python is available; portability is enhanced by the distribution of the software via a conda environment, that seamlessly handles all required dependencies. Additionally, DRONE2REPORT offers ample extendibility allowing users to define new indices or analysis tasks, as shown in the section on software implementation. We also showed how signals from multiple sensors (RGB, multispectral, thermal, DEM) can be integrated to develop custom indices, a feature largely unexplored in existing tools.	741
	742
	743
	744
	745
	746
	747
	748
	749
There are of course a few limitations that need to be pointed out. First of all, there is no graphical interface (GUI), which may pose a barrier for users unfamiliar with command-line tools. This, however, was a design choice, since the tool was developed as part of a larger, server-based pipeline. Moreover, DRONE2REPORT does not currently implement computer vision tasks, e.g. image segmentation or classification. Although the integration of these tools would be trivial (e.g. defining a new [TASK segment]), the application of these techniques is currently outside the scope of the tool.	750
	751
	752
	753
	754
	755
	756
In conclusion, DRONE2REPORT is a new software tool designed to support repeatable, scalable, and multi-sensor UAV data analysis in agricultural field trials, and is going to be of great use and help for the scientific and technical community in precision agriculture and beyond. By focusing on vegetation index calculation, ROI-level analytics, and reproducible reporting, it fills a critical methodological gap between raw imagery and downstream statistical analysis. Its design makes it a valuable asset not only for researchers in precision agriculture, but also for broader applications such as forestry, land-use monitoring, and environmental surveys.	757
	758
	759
	760
	761
	762
	763
	764
<b>Supplementary information.</b>	765
	766
<b>Acknowledgements.</b> We sincerely thank the team Module 7 at the Netherlands Plant Eco-phenotyping Centre (NPEC) at Wageningen University & Research (NL) for the collaboration that sprouted this software.	767
	768
	769
	770
<b>Declarations</b>	771
	772
<b>Funding</b>	773
Funded by the European Union - Next Generation EU, Mission 4, Component 1, CUP B53D23007940006: PRIN 2022 project "Polyploidbreeding 4.0" (G.A.: 2022BACN8A). Also funded by CREA, "stage di mobilità breve all'estero", register number 0107199, 24 november 2023.	774
	775
	776
	777
	778
	779
<b>Competing interests</b>	780
The authors declare that they have no competing interests.	781
	782

783 **Ethics approval and consent to participate**

784 Not applicable.

785

786 **Code availability**

788 **Author contribution**

789

790 **References**

791

- 792 [1] Machwitz, M., Pieruschka, R., Berger, K., Schlerf, M., Aasen, H., Fahrner, S.,  
793 Jiménez-Berni, J., Baret, F., Rascher, U.: Bridging the gap between remote sensing  
794 and plant phenotyping—challenges and opportunities for the next generation  
795 of sustainable agriculture. *Frontiers in plant science* **12**, 749374 (2021)
- 796 [2] Moyroud, N., Portet, F.: Introduction to qgis. *QGIS and generic tools* **1**, 1–17  
797 (2018)
- 798 [3] Tang, H., Kong, W., Nabukalu, P., Lomas, J.S., Moser, M., Zhang, J., Jiang, M.,  
800 Zhang, X., Paterson, A.H., Yim, W.C.: Grabseeds: extraction of plant organ  
801 traits through image analysis. *Plant Methods* **20**(1), 140 (2024)
- 802 [4] Loarca, J., Wiesner-Hanks, T., Lopez-Moreno, H., Maule, A.F., Liou, M., Torres-  
803 Meraz, M.A., Diaz-Garcia, L., Johnson-Cicalese, J., Neyhart, J., Polashock,  
804 J., et al.: Berryportraits: Phenotyping of ripening traits cranberry (*vaccinium  
805 macrocarpon* ait.) with yolov8. *Plant Methods* **20**, 172 (2024)
- 806 [5] Welcome to OpenDroneMap’s documentation — OpenDroneMap 3.5.6 documen-  
807 tation. <https://docs.opendronemap.org/> Accessed 2025-08-27
- 808 [6] Rupnik, E., Daakir, M., Pierrot Deseilligny, M.: Micmac—a free, open-source solu-  
809 tion for photogrammetry. *Open geospatial data, software and standards* **2**(1), 14  
810 (2017)
- 811 [7] GDAL/OGR contributors: GDAL/OGR Geospatial Data Abstraction Software  
812 Library. Open Source Geospatial Foundation, (2025). <https://doi.org/10.5281/zenodo.5884351>. Open Source Geospatial Foundation. <https://gdal.org>
- 813 [8] Jordahl, K., Bossche, J.V., Fleischmann, M., Wasserman, J., McBride, J., Gerard,  
814 J., Tratner, J., Perry, M., Badaracco, A.G., Farmer, C., Hjelle, G.A., Snow,  
815 A.D., Cochran, M., Gillies, S., Culbertson, L., Bartos, M., Eubank, N., maxalbert,  
816 Bilogur, A., Rey, S., Ren, C., Arribas-Bel, D., Wasser, L., Wolf, L.J., Journois, M.,  
817 Wilson, J., Greenhall, A., Holdgraf, C., Filipe, Leblanc, F.: Geopandas/geopan-  
818 das: V0.8.1. <https://doi.org/10.5281/zenodo.3946761>. <https://doi.org/10.5281/zenodo.3946761>
- 819 [9] Louhaichi, M., Borman, M.M., Johnson, D.E.: Spatially located platform and  
820 aerial photography for documentation of grazing impacts on wheat. *Geocarto  
821 International* **36**(1), 1–12 (2021)
- 822
- 823
- 824
- 825
- 826
- 827
- 828

International <b>16</b> (1), 65–70 (2001)	829
	830
[10] Hamuda, E., Glavin, M., Jones, E.: A survey of image processing techniques for plant extraction and segmentation in the field. Computers and electronics in agriculture <b>125</b> , 184–199 (2016)	831
	832
	833
	834
[11] Mathieu, R., Pouget, M., Cervelle, B., Escadafal, R.: Relationships between satellite-based radiometric indices simulated using laboratory reflectance data and typic soil color of an arid environment. Remote sensing of environment <b>66</b> (1), 17–28 (1998)	835
	836
	837
	838
[12] Meyer, G.E., Neto, J.C.: Verification of color vegetation indices for automated crop imaging applications. Computers and electronics in agriculture <b>63</b> (2), 282–293 (2008)	839
	840
	841
	842
[13] Henrich, V., Krauss, G., Götze, C., Sandow, C.: Idb - www.indexdatabase.de, entwicklung einer datenbank für fernerkundungsindizes. Bochum: AK Fernerkundung <b>15</b> (2012)	843
	844
	845
	846
[14] Virtanen, P., Gommers, R., Oliphant, T.E., Haberland, M., Reddy, T., Cournapeau, D., Burovski, E., Peterson, P., Weckesser, W., Bright, J., van der Walt, S.J., Brett, M., Wilson, J., Millman, K.J., Mayorov, N., Nelson, A.R.J., Jones, E., Kern, R., Larson, E., Carey, C.J., Polat, İ., Feng, Y., Moore, E.W., VanderPlas, J., Laxalde, D., Perktold, J., Cimrman, R., Henriksen, I., Quintero, E.A., Harris, C.R., Archibald, A.M., Ribeiro, A.H., Pedregosa, F., van Mulbregt, P., SciPy 1.0 Contributors: SciPy 1.0: Fundamental Algorithms for Scientific Computing in Python. Nature Methods <b>17</b> , 261–272 (2020) <a href="https://doi.org/10.1038/s41592-019-0686-2">https://doi.org/10.1038/s41592-019-0686-2</a>	847
	848
	849
	850
	851
	852
	853
	854
	855
	856
[15] Nelder, J.A., Mead, R.: A simplex method for function minimization. The computer journal <b>7</b> (4), 308–313 (1965)	857
	858
	859
[16] Tanaka, T.S.T., Wang, S., Jørgensen, J.R., Gentili, M., Vidal, A.Z., Mortensen, A.K., Acharya, B.S., Beck, B.D., Gislum, R.: Review of Crop Phenotyping in Field Plot Experiments Using UAV-Mounted Sensors and Algorithms. Drones <b>8</b> (6), 212 (2024) <a href="https://doi.org/10.3390/drones8060212">https://doi.org/10.3390/drones8060212</a> . Accessed 2025-08-27	860
	861
	862
	863
	864
[17] Gano, B., Bhadra, S., Vilbig, J.M., Ahmed, N., Sagan, V., Shakoor, N.: Drone-based imaging sensors, techniques, and applications in plant phenotyping for crop breeding: A comprehensive review. The Plant Phenome Journal <b>7</b> (1), 20100 (2024)	865
	866
	867
	868
	869
[18] Gano, B., Bhadra, S., Vilbig, J.M., Ahmed, N., Sagan, V., Shakoor, N.: Drone-based imaging sensors, techniques, and applications in plant phenotyping for crop breeding: A comprehensive review. The Plant Phenome Journal <b>7</b> (1), 20100 (2024) <a href="https://doi.org/10.1002/ppj2.20100">https://doi.org/10.1002/ppj2.20100</a> . Accessed 2025-08-27	870
	871
	872
	873
	874

- 875 [19] Sharma, M., Raghavendra, S., Agrawal, S.: Development of an open-source tool  
876 for uav photogrammetric data processing. Journal of the Indian Society of Remote  
877 Sensing **49**(3), 659–664 (2021)
- 878
- 879 [20] Vacca, G., *et al.*: Web open drone map (webodm) a software open source to  
880 photogrammetry process. In: Fig Working Week 2020. Smart Surveyors for Land  
881 and Water Management, (2020)
- 882
- 883 [21] Orfeo ToolBox – Orfeo ToolBox is not a black box. <https://www.orfeo-toolbox.org/> Accessed 2025-08-27
- 884
- 885 [22] Grizonnet, M., Michel, J., Poughon, V., Inglada, J., Savinaud, M., Cresson, R.:  
886 Orfeo ToolBox: open source processing of remote sensing images. Open Geospatial  
887 Data, Software and Standards **2**(1), 15 (2017) <https://doi.org/10.1186/s40965-017-0031-6> . Accessed 2025-08-27
- 888
- 889
- 890 [23] Dobesova, Z.: Evaluation of effective cognition for the qgis processing modeler.  
891 Applied Sciences **10**(4), 1446 (2020)
- 892
- 893 [24] PlantCV (2021). <https://plantcv.org> Accessed 2025-08-27
- 894
- 895 [25] Varghese, R., Sambath, M.: Yolov8: A novel object detection algorithm with  
896 enhanced performance and robustness. In: 2024 International Conference on  
897 Advances in Data Engineering and Intelligent Computing Systems (ADICS), pp.  
898 1–6 (2024). IEEE
- 899
- 900 [26] Matias, F.I., Caraza-Harter, M.V., Endelman, J.B.: FIELDimageR: An R package  
901 to analyze orthomosaic images from agricultural field trials. The Plant Phenome  
902 Journal **3**(1), 20005 (2020) <https://doi.org/10.1002/ppj2.20005> . Accessed 2025-  
903 08-27
- 904
- 905 [27] Candiago, S., Remondino, F., De Giglio, M., Dubbini, M., Gattelli, M.: Evaluating  
906 multispectral images and vegetation indices for precision farming applications  
907 from uav images. Remote sensing **7**(4), 4026–4047 (2015)
- 908
- 909 [28] Radočaj, D., Šiljeg, A., Marinović, R., Jurišić, M.: State of major vegetation  
910 indices in precision agriculture studies indexed in web of science: A review.  
911 Agriculture **13**(3), 707 (2023)
- 912
- 913 [29] Vélez, S., Martínez-Peña, R., Castrillo, D.: Beyond vegetation: A review unveiling  
914 additional insights into agriculture and forestry through the application of  
915 vegetation indices. J **6**(3), 421–436 (2023)
- 916
- 917
- 918
- 919
- 920